Identifying small pelagic Mediterranean fish schools from acoustic and environmental data using optimized artificial neural networks

S. Aronica[a,1], I. Fontana[a,1], G. Giacalone[a,1], G. Lo Bosco[b,*,1], R. Rizzo[c,1], S. Mazzola[a], G. Basilone[a], R. Ferreri[a], S. Genovese[a], M. Barra[a], A. Bonanno[a]

[a] IAMC–CNR, National Research Council of Italy, Torretta Granitola, Trapani, Italy
[b] DMI, University of Palermo, Via Archirafi, Palermo, Italy
[c] ICAR–CNR, National Research Council of Italy, Via Ugo La Malfa, Palermo, Italy

ARTICLE INFO

ABSTRACT

The Common Fisheries Policy of the European Union aims to exploit fish stocks at a level of Maximum Sustainable Yield by 2020 at the latest. At the Mediterranean level, the General Fisheries Commission for the Mediterranean (GFCM) has highlighted the importance of reversing the observed declining trend of fish stocks. In this complex context, it is important to obtain reliable biomass estimates to support scientifically sound advice for sustainable management of marine resources. This paper presents a machine learning methodology for the classification of pelagic species schools from acoustic and environmental data. In particular, the methodology was tuned for the recognition of anchovy, sardine and horse mackerel. These species have a central role in the fishing industry of Mediterranean countries and they are also of considerable importance in the trophic web because they occupy the so-called middle trophic level. The proposed methodology consists of a classifier based on an optimized two layer feed-forward neural network. Morphological, bathymetric, energetic and positional features, extracted from acoustic data, are used as input, together with other environmental data features. The classifier uses an optimal number of neurons in the hidden layer, and a feature selection strategy based on a genetic algorithm. Working on a dataset of 2565 fish schools, the proposed methodology permitted us to identify the these three fish species with an accuracy of around 95%.

1. Introduction

The small pelagic fish species, such as European anchovy (*Engraulis encrasicolus*), European sardine (*Sardina pilchardus*) and horse mackerel (*Trachurus trachurus*), play an important socio-economic role and they constitute more than one third of sea fishing overall (FAO, GFCM, 2016). For this reason, they are included in a category of considerable importance in the fishing industry and in the international canning industry operating in the fisheries sector (FAO, GFCM, 2016; Lleonart & Maynou, 2003). Furthermore, small pelagics are of considerable importance in the trophic web because they occupy the so–called middle trophic level (Rumolo et al., 2016, 2017, 2018) between the base of the trophic chain (phytoplankton/zooplankton) and the predators (Cury et al., 2000, 2003; Pauly et al., 1998). Thus, these species play a fundamental role in energy transfers from primary producers to final consumers (Preciado et al., 2008; Morote et al., 2008). Mainly for anchovy and sardine, many authors have highlighted how these short-

living species are characterized by large interannual fluctuations in the biomass (Crawford, 1987; Schwartzlose & Alheit, 1999; Palomera et al., 2007; Basilone et al., 2017, 2018; Bonanno et al., 2018). In the years when the levels of biomass are low, the effect of a high fishing effort would lead to a collapse of these resources even from one year to another. The collapse of these species has been well-documented in the literature showing that the recovery times are very long and can have catastrophic socio–economic impacts on the seafaring communities that live thanks to the income from fishing and marketing of canned products (Gascuel, 2005; Pauly et al., 2002; Jackson et al., 2001; Cooke, 1984). At the Mediterranean level, where such species are shared among different fisheries belonging to different countries, there is a clear awareness that these resources should be sustainably exploited (FAO, GFCM, 2016).

Nevertheless, in the last years, Mediterranean fisheries have faced serious challenges, with roughly 85% of the scientifically assessed fish stocks considered to be fished outside biologically sustainable limits

---

* Corresponding author at: DMI, University of Palermo, Via Archirafi, Palermo, Italy
  E-mail address: giosue.lobosco@unipa.it (G. Lo Bosco).
[1] These authors contributed equally to this work.
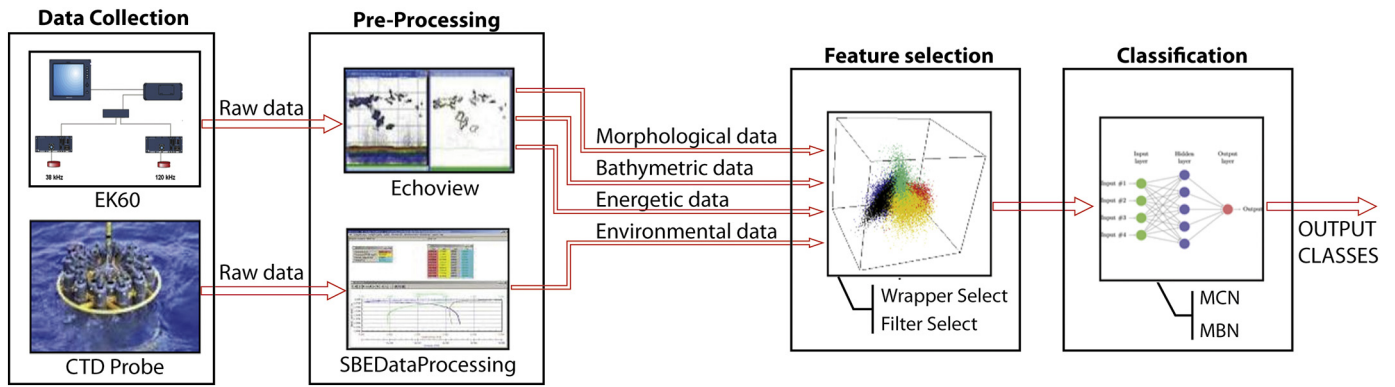
Fig. 1. The workflow of the proposed methodology.

(FAO, GFCM, 2016). The General Fisheries Commission for the Mediterranean (GFCM), through the Resolution GFCM/40/2016/2 for a mid-term strategy (2017–2020), singled out the importance of reversing the declining trend of fish stocks through strengthened scientific advice in support of management. Furthermore, the Common Fisheries Policy (CFP) of the European Union aims to exploit fish stocks at a level of Maximum Sustainable Yield (MSY) by 2020 at the latest. In this complex context, it is essential to obtain reliable biomass estimates to support scientifically sound advice for sustainable management of marine resources. This is especially relevant in a highly dynamic environment such as the central Mediterranean sea where hydrology strongly influences the variability in primary production as well as in the other levels of the pelagic food web (Valenti et al., 2012; Bonanno et al., 2015, 2016). The most common and adopted method for estimating small pelagic biomass and distribution is the acoustic method (Simmonds & MacLennan, 2008). The combined use of acoustic data, acquired along transects according to a specific survey design (Barra et al., 2015), and experimental catches through a pelagic net permit us to evaluate biomasses of the target fish species in small or broad sea areas (Bonanno et al., 2015, 2016). The allocation of acoustic backscattered energy to different pelagic species can be performed in various ways (Petitgas et al., 2003). One of the most sensitive aspects of the acoustic method for biomass estimation is the species identification of insonified fish schools, which can be performed either by trawl sampling or by scrutinizing the echograms; that is, applying expert criteria and considering additional information such as school distribution and behavioural patterns (Simmonds & MacLennan, 2008; Horne, 2000; Martignac et al., 2015; Kloser et al., 2002). However, these techniques, in addition to being time-consuming, may result in considerable variations of the biomass estimates in relation to the experience of the scrutinizer expert (Tsagarakis et al., 2015). Incorrect pelagic fish species classification can limit the reliability of acoustic abundance estimates. Therefore, the objective species identification directly from acoustic data may give a significant contribution to the reliability of acoustic abundance estimates without any human error during the data analysis (Lawson et al., 2001).

In previous studies, statistical models were applied to directly identify different species present in small pelagics assemblages. For example, a statistical spectral method has been proposed for echo classification of data in the Southern California Bight coastal area (Demer et al., 2009). Moreover, a Classification–Trees approach for species identification of fish–school echo-traces in the North Sea was adopted (Fernandes, 2009). Several studies have used school descriptors extracted from acoustic data to classify species. The descriptors are generally divided into four categories: morphological (e.g., geometry of the school), bathymetric (e.g., position of the school in the water column), energetic (e.g., properties of the backscattered signal), and positional (e.g., offshore distance of the school) (Robotham et al., 2010; Scalabrin, 1991; Scalabrin & Massé, 1993; Reid, 1999;

Campanella & Taylor, 2016). In the Mediterranean sea, Campanella et al. (D'Elia et al., 2014) identified various sub-groups of anchovies, sardines, horse mackerels and other pelagic species (OPS), mainly taking into account the bathymetric, energetic and morphologic features of fish schools; the authors used Classification Trees, reaching an accuracy on 75% of the cases. In other studies, has emerged that the classification methods through heuristic approaches, such as neural networks, offer different results depending on the used data type. For example, Robotham et al. (Robotham et al., 2010) and Charef et al. (Charef et al., 2010) reached a percentage of successful classification of around 87% and 89%, respectively, selecting proper subsets of acoustic features. In Fontana et al. (Fontana et al., 2017) the authors applied a PNN neural network for discriminating groups of sardines and anchovies and taking into account only the morphological and energetic parameters of schools. The percentage of successful classification was on average about 74%. In this paper, a machine learning methodology is applied to identify fish schools of three small pelagic fish species: anchovy, sardine and horse mackerel. One of the novelties of this paper, compared to others in the literature, regards the combined use of environmental and acoustic features. A comparison between two methodologies, which take into account a three–classes species classifier and a combination of binary species classifiers, was also performed for the final classification scheme to be adopted.

2. Materials and methods

The computational methodology adopted for the automatic identification of pelagic fish species is schematized in Fig. 1. The identification problem is reduced to a classification task, which is performed by using a machine learning methodology. In the following, each block of the workflow is described in detail.

2.1. Data collection

The collected data were acquired during 16 acoustic surveys carried out between 2005 and 2015 in the central Mediterranean Sea. In particular, 11 surveys were carried out in the Strait of Sicily and five surveys along the Italian coasts of the Tyrrhenian Sea (Fig. 2). The surveys were all performed during the summer between June and September. The acoustic data were collected using a Simrad EK60 scientific echo-sounder, equipped with two hull–mounted split-beam transducers operating at 38 and 120 kHz. The current scientific echo-sounders, available in the market, are unable to directly recognize species composition of the fish schools met during a typical echo survey. Consequenlty, the acoustic data acquisition phase is integrated by a biological sampling phase through a pelagic trawl net. In this way, for each trawl haul, it is possible to obtain both species composition and size distribution of the insonified fishes. The adoption of the nearest haul method (Petitgas et al., 2003) may permit us to merge the
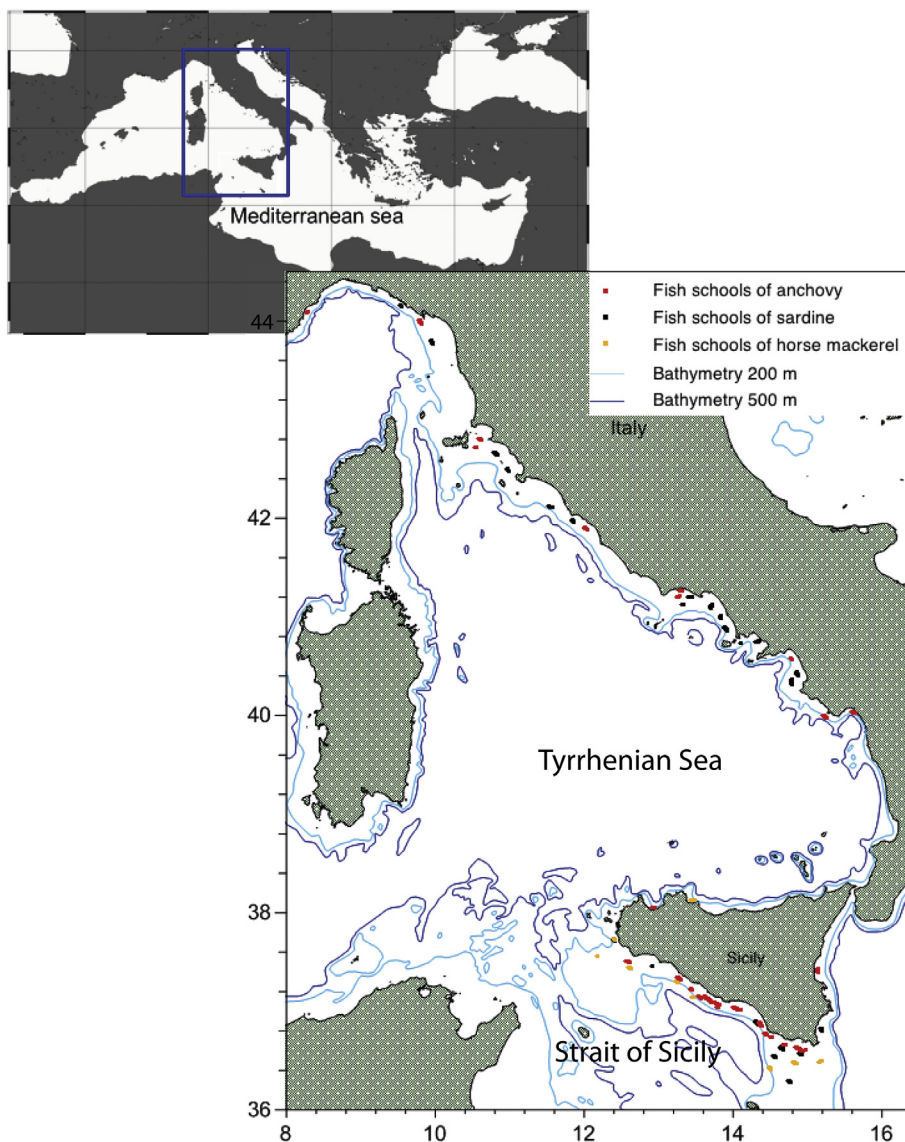
Fig. 2. The figure shows the position of the anchovy (red), sardine (black) and horse mackerel (orange) schools respectively associated with monospecific hauls. (For interpretation of the references to colour in this figure legend, the reader is referred to the web version of this article.)
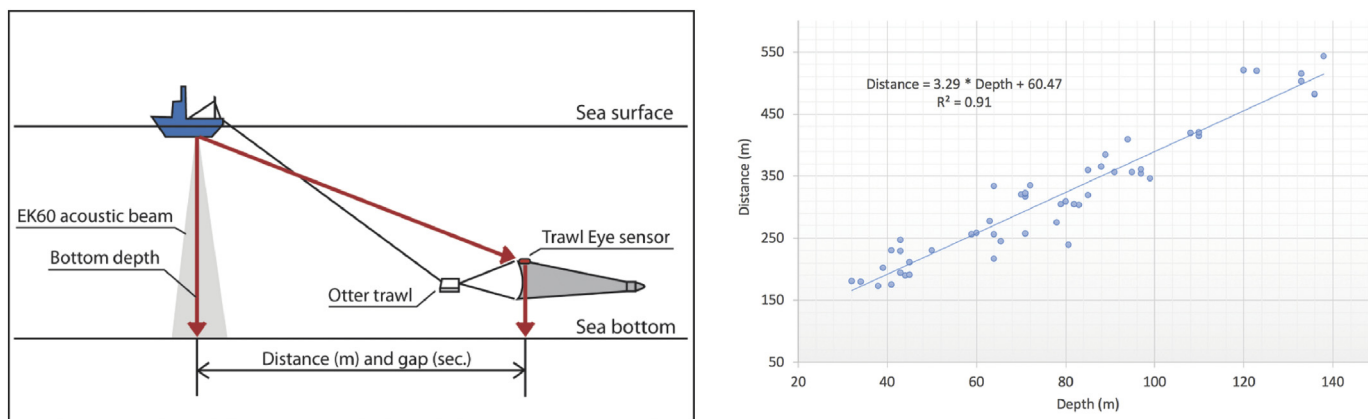
Fig. 3. Schematic view of the relative positions of the vessel and the pelagic trawl net (left-hand panel). Scatterplot between the sea bottom depth and the distance between the pelagic trawl net and the ITI hull-mounted transducers (right-hand panel).

biological and acoustic data, and to obtain small pelagic fish density (t/nm^2) for each nautical mile, irrespective of the echo traces (Bonanno et al., 2018). The pelagic trawl net used to allow a direct match between the catch and the echograms for the validation of the acquired data has a horizontal opening of 13 ÷ 15 m, vertical mouth opening of 6 ÷ 9 m and a mesh size of 10 mm in the cod–end (Charef et al., 2010; Cabreira et al., 2009). The echograms were acquired during diurnal trawl hauls, and the entire dataset was built considering only the monospecific catches of anchovy (EE — *Engraulis encrasicolus*), sardine (SP — *Sardina pilchardus*) and horse mackerel (TT — *Trachurus trachurus*). For the aim of this study, only those trawl hauls where 80% of the catch (with a minimum weight of 5 kg) comprised the same species were considered as monospecific hauls. During the trawl hauls considered in the present study, the distance between the EK60 hull-mounted transducers and the net ranged between 170 and 540 m. Consequently, the time interval between the echo sounder beam and the trawl net ranged between 83 and 262 s, considering a typical vessel speed of about 4 knots during the trawl haul (Fig. 3). For this method, which is typically adopted in field experiments (D'Elia et al., 2014; Charef et al., 2010; Cabreira et al., 2009), this is a technical limitation that cannot be overcome at the moment with the available devices and, consequently, the described procedure is the only one that is adopted during an acoustic survey at sea. During daylight, pelagic fish schools are located very close to the bottom (D'Elia et al., 2014). For this reason, to reduce the effects of escaping behaviour of fishes, during the trawl operations the net is positioned very close to the bottom. In the present study, the following single–species trawl hauls were analyzed: 21 hauls with 1164 EE schools, 22 hauls with 1160 SP schools and 11 hauls with 241 schools of TT. During the surveys, monospecific trawl hauls of other pelagic species have never been met. The vertical profiles of the main physical–chemical parameters of the water column were acquired through a multi-parameter CTD probe SBE911 (Sea-Bird Inc., 13,431 NE 20th Street, Bellevue, Washington 98,005 USA). The probe was equipped with sensors for monitoring temperature, salinity, fluorescence and oxygen. CTD profiles were collected during the survey according to the MEDIAS (MEDiteranean International Acoustic Survey) protocol which foresees that" Since the environmental parameters are very important for small pelagic fish, a minimum of 3 CTD stations should be held per transect or a grid of stations with density adequate to describe the oceanography of the surveyed area".

In Fig. 4, the acoustic survey design and the position of the CTD stations in the Tyrrhenian Sea and in the Strait of Sicily are shown.

2.2. Preprocessing

The analysis of acoustic data at 38 kHz and 120 kHz was carried out with the Myriax Software Pty Ltd.'s Echoview (Higginbottom, 2000); the adopted workflow was structured in two consecutive steps. In the first step, the removal of background noise from the echograms of both frequencies was performed by using the method proposed in (De Robertis & Higginbottom, 2007). This is a simple post-processing technique that assumes that background noise dominates some part of the acoustic signal, in which the backscattered signal has a negligible contribution. If this assumption is met, then the method can provide robust and accurate estimates of background noise. The estimated background noise is then removed from the echograms by using simple mathematical operators. Due to the different acoustic power values transmitted by the two transducers (2000 W at 38 kHz and 250 W at 120 kHz) and the different seawater absorption for the two frequencies, the effects of background noise are more evident in echograms at 120 kHz. Taking into account the large area covered during the echo surveys, from shallow waters to offshore areas, from the Strait of Sicily (mean latitude 37° N) to the Ligurian sea (mean latitude 43° N), with different background noise levels, it was decided to adopt an objective approach to analyze the whole acoustic dataset. Consequently, the workflow adopted in this study foresaw the removal of background noise from the echograms of both frequencies. On the virtual echograms, which were obtained by summing echograms of the two frequencies, two convolution kernels were applied, characterized by a median filter (3 × 3) and a dilation filter (5 × 5), respectively. This approach permitted us to remove individual (small) samples, in agreement to (Fernandes, 2009). Finally, the use of a threshold of −116 dB permitted us to obtain a binary mask to be applied to the original 38 kHz echogram (D'Elia et al., 2014; MEDIAS-Handbook, 2015). In the second step, candidate fish schools were detected and isolated from the masked 38 kHz echograms using the SHAPES algorithm, implemented in Echoview (Barange, 1994). The detection parameters that we used were: minimum total school length of 10 m, minimum school height of 1 m, minimum candidate length of 5 m, minimum candidate height of 1 m, a maximum vertical linking distance of 2 m, and maximum horizontal linking distance of 5 m. The two linking distances are the vertical and horizontal semi-axes of an ellipse. The ellipse is moved around the boundary of a school candidate. If any part of any other school candidate falls within the oval, a link is created between the school candidates (Kang, 2011). Fig. 5 shows an example of an echogram in which *Engraulis encrasicolus* schools were identified. For each identified fish school, it was possible to extract a set of descriptors grouped into four categories: morphological (parameters that characterize the shape of the bench), energetic (parameters derived from backscattered signals), bathymetric (position of the school in the water column) and positioning (distance from the coast). Table 1 shows the complete list of the features extracted for each school. More information on the meaning of the individual parameters is reported in Table 10. The school position with respect to the coast was calculated by determining the distance between the school coordinates and the coordinates of the nearest point of the coastline.

The collected CTD profiles data were processed using SEASOFT-WIN32 software, according to the Mediterranean and Ocean Data Base Instructions (Brankart, 1994). For each identified fish school, the environmental parameters of the nearest CTD profile have been associated by taking into account the values acquired near the sea surface (typically 5 m) and the bottom.

2.3. Feature selection

Feature selection is fundamental to the success of many real–world applications of machine learning techniques. The primary goal of feature selection algorithms is to speed-up the response of the machine learning model and to reduce the presence of noise features or low significance features. In classification tasks, like the one described in this work, feature selection is the search for an element (subset) of the partition set of the feature set that optimizes the classification performances. In many real cases, the feature selection is a computationally intractable problem, and its solution needs a proper heuristic (Kohavi & John, 1997). Mainly, there are two classes of feature selection methods: the *filter approaches*, which score the subset by looking at the intrinsic properties of data, and the so-called *wrapper approaches*, which use a predictive model (often the classification model itself) to evaluate the feature subset (Guyon & Elisseeff, 2003).

The main difference between the two methods is on running time, encouraging the filter versus the wrapper; conversely, the wrapper has demonstrated to be more accurate. In this work, one filter and one wrapper approach have been adopted. In the following subsections, these two methods will be described.

2.3.1. The filter approach

The filter approach that we adopted, named *filter select* (FS for short) is based on the feature statistics, and it applies in the case of a binary label assignment of a dataset. The method is described in Chapter 5 of the book by Theodoridis et al. (Theodoridis & Koutroumbas, 2008). The binary labels identify two paired samples for each features j, and the absolute value z_j of the difference between the feature means of the two
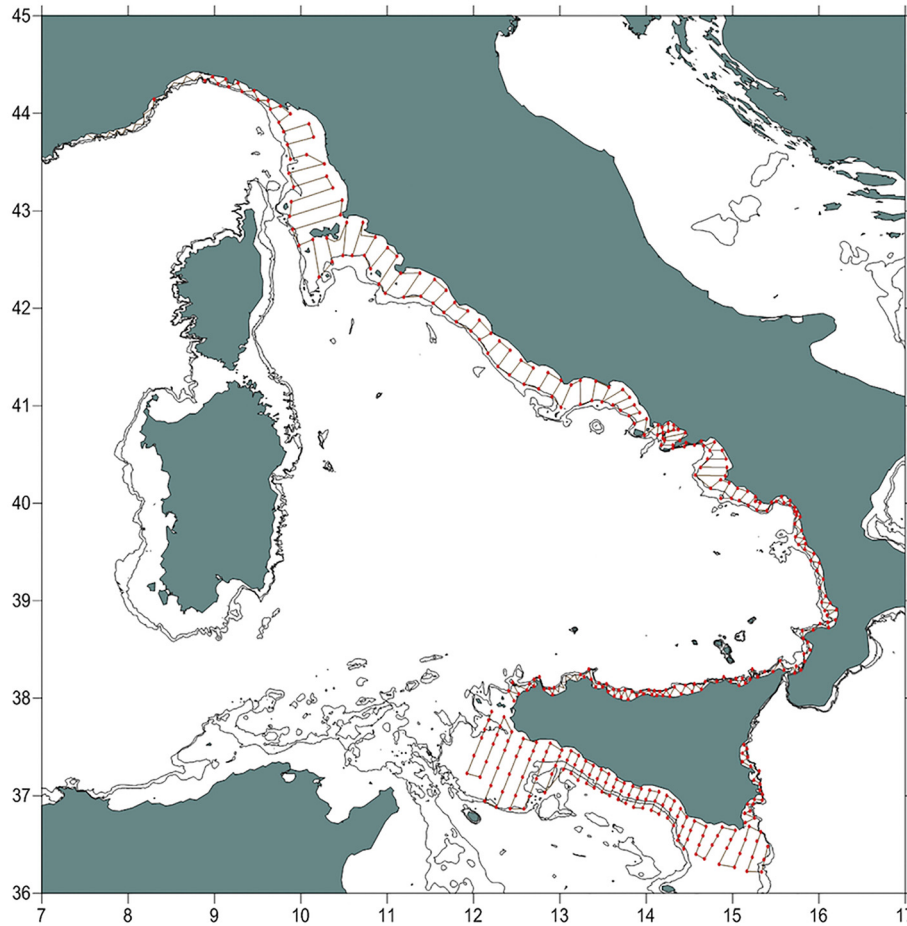
Fig. 4. Acoustic survey design (brown lines) and position of the CTD stations (red dots) in the surveyed areas. (For interpretation of the references to colour in this figure legend, the reader is referred to the web version of this article.)
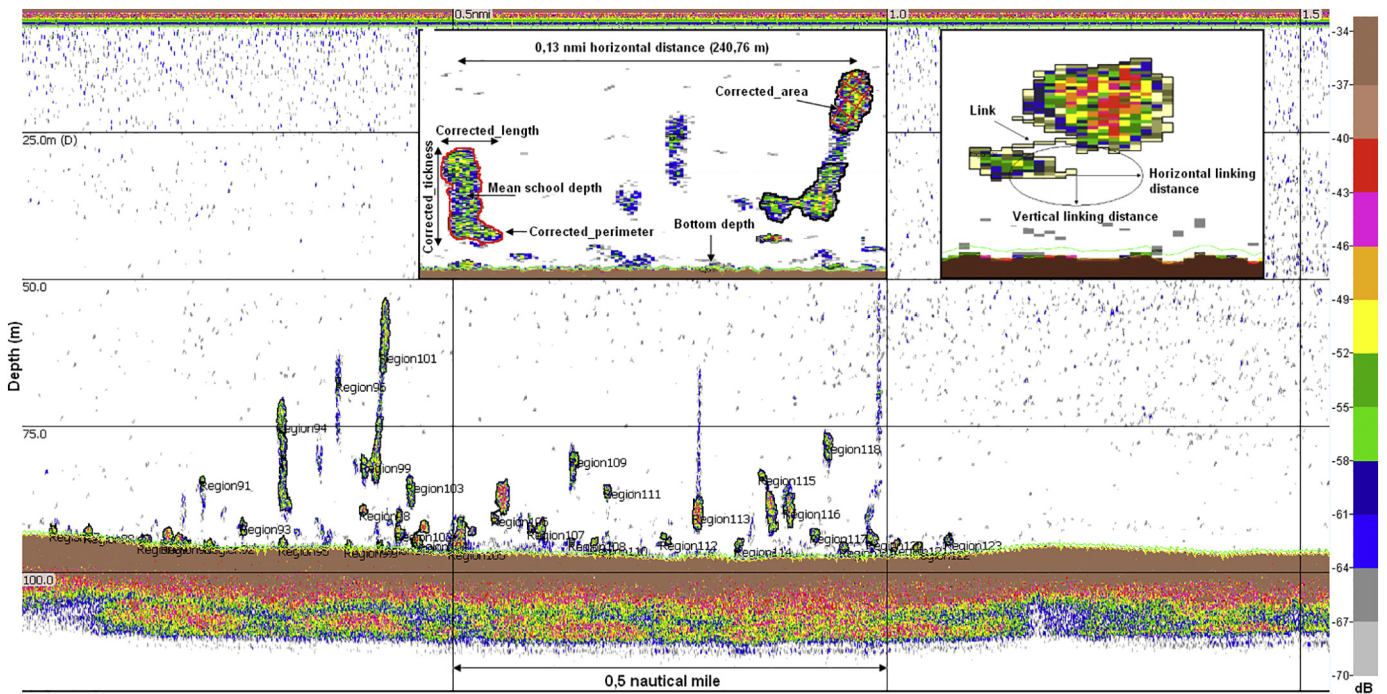
Fig. 5. Typical echogram acquired during an echo survey. The use of the SHAPE algorithm permitted to evidence the candidate fish school (labelled "region"). The right-hand panel evidences some details of such algorithm; in this case, two candidate fish schools are considered to belong to a single fish school. Some of the features listed in Table 1 are visible in the central panel. The colour scale for the Sv values is shown on the right side of the figure.

Table 1
The list of extracted features.

Type	No.	Descriptor	Units	Type	No.	Descriptor	Units
Morphological	1	Kurtosis	dB re 1 m^{-1}		21	Height_mean	m
	2	Attack_angle	°		22	Standard_deviation	
	3	Corrected_length	m		23	Skewness	dB re l m^{-1}
	4	Corrected_thickness	m	**Energetic**	24	Sv_mean	dB re l m^{-1}
	5	Corrected_perimeter	m		25	Sv_max	dB re l m^{-1}
	6	Corrected_area	m^2		26	Sv_min	dB re l m^{-1}
	7	Image_compactness			27	Sv_noise	dB re l m^{-1}
	8	Corrected_mean_amplitude	m^2/m^3		28	Nasc	m2/nmi^2
	9	Corrected MVBS	dB re 1 m^2/m^3		29	ABC	m2/nmi^2
	10	Coefficient of variation	%	**Bath**	30	Mean school depth	m
	11	Horizontal roughness coefficient	dB re 1 m^2/m^3		31	Bottom depth	m
	12	Vertical_roughness_coefficient	dB re 1 m^2/m^3	**Pos**	32	Distance from the coast	nmi
	13	3D_school_area	m^2		33	Water temperature at 5 m	deg C
	14	3D_schoo1_volume	m^3	**Environmental**	34	Water temperature at the bottom	deg C
	15	Area_backscatter_strength	m^2/nmi^2		35	Salinity at 5 m	PSU
	16	Density_number	fish/nmi^2		36	Salinity at the bottom	PSU
	17	Density_weight	kg/nmi^2		37	Fluorescence at 5 m	ug/1
	18	Thickness_mean	m		38	Fluorescence at the bottom	ug/1
	19	Range_mean	m		39	Oxygen at 5 m	mg/1
	20	Beam_volume_sum	m^3		40	Oxygen at the bottom	mg/1

sample, normalized by the sum of the variances, is used for the selection. Thus, high values of z_j favours the selection of the feature j. Each z_j is then weighed by weight w_j so defined

$$w_j = z_j*(1 - \alpha*\rho_j) \tag{1}$$

where ρ_j is the average of the absolute values of the pearson correlations between the candidate feature j and the others. The value α sets the weighting factor by a scalar value between 0 and 1. When $\alpha = 0$ potential features are not weighted. A value of $\rho \approx 1$ reduces the weight of the features that are highly correlated with the others. The final output of FS is a ranking of the overall set of features, accordingly to the values of the weights w. The implementation details and parameters values that will be used for the experiments will be discussed in Section 3.2.1.

2.3.2. The wrapper approach

The wrapper approach is referred to as *wrapper select* (WS for short). In the general framework of wrapper approaches, an algorithm generates a candidate solution for the feature selection problem, and an evaluation function is used to test its quality (Huan & Motoda, 1998). Taking into consideration that the feature selection can be configured as an optimization problem, one possible solution is to use a genetic algorithm (GA for short) to generate a pool of candidate solutions and to use the performances of the classification algorithm as fitness function (Tsai et al., 2013).

Given that an input sample is a vector in $\Re^m$ ($\vec{x_i} \in \Re^m$), a candidate solution of the feature selection problem can be represented as a mask vector $\vec{s} \in \{0,1\}^m$ where each component $s_j \in \{0,1\}$ and $s_j = 1$ means that the feature j is present in the set of the selected features. Each mask vector $\vec{s}$ defines a function f_s that maps each $\vec{x_i} \in \Re^m$ into a vector

$$f_s(\vec{x_i}) = \vec{z_i} \in \Re^r \tag{2}$$

with

$$m > r = \sum_{j=1}^{m} s_j \tag{3}$$

The GA will operate on a population of masks vectors S, and the goal will be the optimization of the accuracy of the classification algorithm that processes the masked data vectors. The implementation details and the parameter values of the GA will be discussed in Section 3.2.2.

2.4. Classification

The adoption of a proper classifier depends on the specific

classification problem, in this case, a feed-forward neural network with a single hidden layer, was adopted as a classification algorithm. In contrast to other classifiers, feed–forward neural networks are characterized by the so–called universal property of the neural network (Hornik et al., 1989) which states that a feed–forward network with a single hidden layer containing a finite number of neurons can approximate each continuous functions on compact subsets of n–tuples of real numbers, under mild assumptions on the activation functions. Consequently, this general topology was adopted as a base for the classifiers. In this work, two different classifier architecture were considered for the pelagic species identification. The first, which is named *multiclass–neural* (MCN for short) is a feed-forward neural network with $m = 40$ inputs, one hidden layer with K neurons and three outputs, each representing the probability that a fish belongs to the corresponding class (see Fig. 6(a)). The second architecture uses the paradigm of the combination of binary classifiers, and is indicated as *multibinary–neural* (MBN for short). This classifier is a combination of three binary classifiers B_h, each using class h as a class of positives, (h = EE, SP or TT), and $\cup_{j \neq h} j$ as a class of negatives, indicated as other pelagic species (OPS for short, see Fig. 6(b)). Each classifier B_h is a feed forward neural network with one hidden layer of K units, m inputs and two outputs each giving the probabilities $p_h(x)$ and $q_h(x)$ of an input sample x of being and not being of class h respectively. Let I be the indicator function of a predicate P, i.e. $I(P) = 1$ if P is true, otherwise $I(P) = 0$. If a function

$$f(h,x) = I(p_h(x) > q_h(x)) * p_h(x) \tag{4}$$

is defined, then setting also:

$$f(OPS,x) = \prod_{h=EE,SP,TT} I(p_h(x) < q_h(x)) \tag{5}$$

the combination paradigm assign to x the final class

$$c(x) = argmax_{k=EE,SP,TT,OPS}(f(k,x)) \tag{6}$$

The definition of the combination strategy states that the species h of an unknown element x is assigned to the one with the higher positive probability ($p_h(x)$) greater than corresponding negative ($p_h(x) > q_h(x)$), otherwise to the OPS class in the case that no positive probabilities are greater than corresponding negatives ($p_h(x) < q_h(x)$ for each h). The possibility to identify an *unknown class* of fish (OPS) with respect to the three considered one is a useful property that characterizes the MBN classifier vs the MCN one.
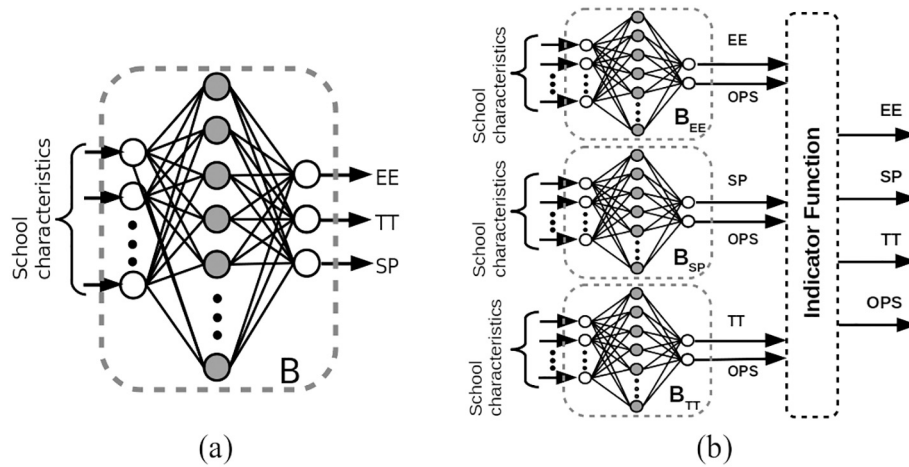
Fig. 6. Outline of the two classifiers: (a) Multiclass-neural on the left and (b) Multibinary-neural on the right. In gray there are the K hidden units.
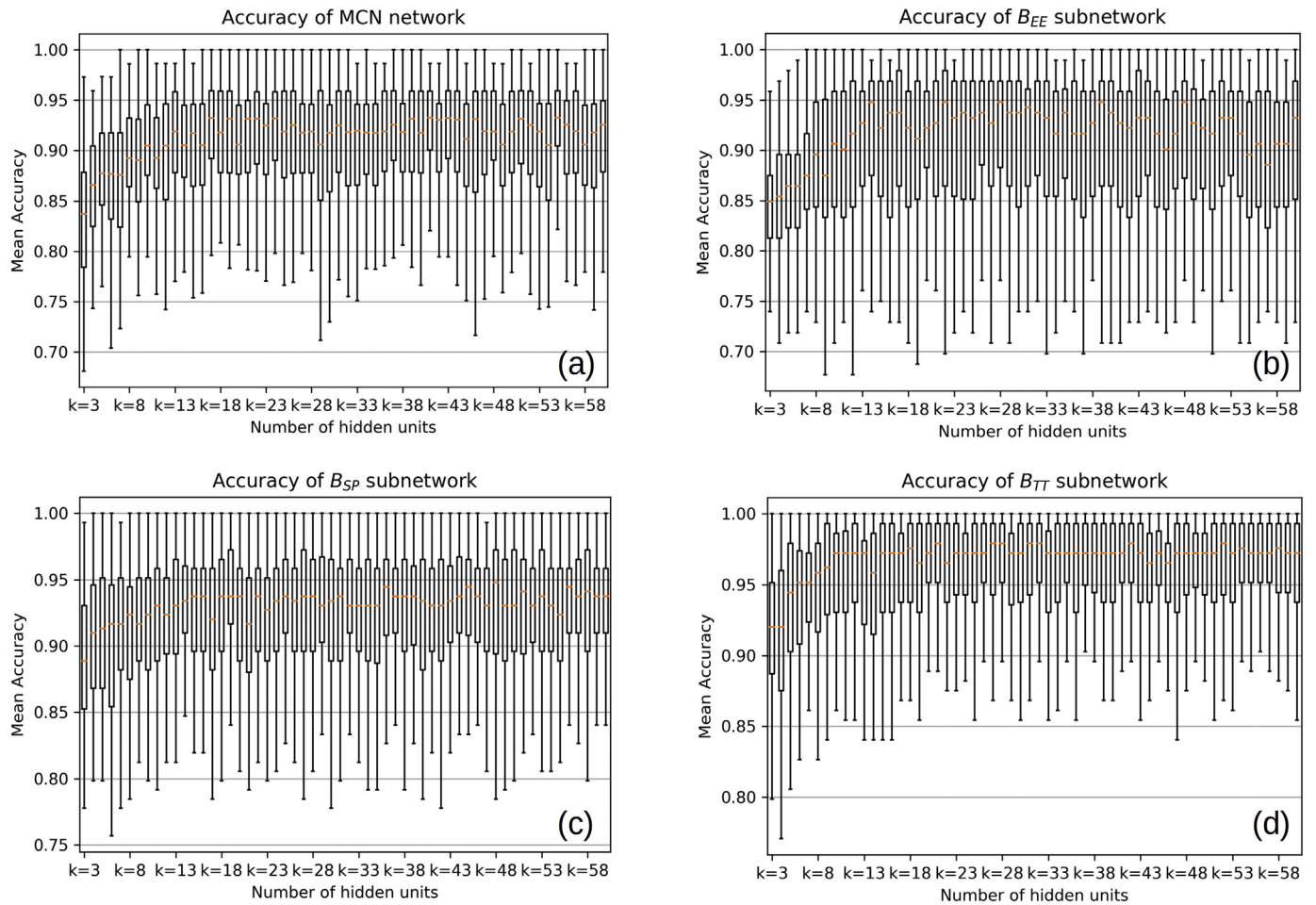
Fig. 7. Boxplots of the accuracies of the classifiers for each number of hidden units K. In the subfigure (a) the accuracy of the MCN classifier. In the other subfigures the performance of each binary classifier that will be part of the MBN classifier: B_{EE}, in subfigure (b), B_{SP}, in subfigure (c) and B_{TT}, in subfigure (d). In plots (b), (c) and (d) of the binary classifiers OPS stands for Other Pelagic Species.

3. Experimental results

The goal of this work is to provide a suitable classifier for the identification of pelagic species. To this purpose, two different neural network classifiers has been considered, the MCN and the MBN. The experiments have been performed in two stages. In the first one, a proper estimation of the number of neurons in the hidden layer has

been carried out. The second stage is devoted to the selection of the subset of features, using filter and wrapper approaches. The following parameters were used for both the sets of experiments involving the two neural networks:

- General topology of the network:
  - Two levels (one hidden)

- Activation functions for the first level: *sigmoids*
- Activation functions for the second level: *softmax*
- Performance funcion: *crossentropy*, no regularization
- Learning algorithm: Scaled conjugate gradient backpropagation, with the following parameters:
  - $Min - grad = 1 \times 10^{-6}$ (minimum performance gradient before training is stopped)
  - $Validation - checks = 10$ (maximum Validation Checks before training is stopped).
  - $\sigma = 5.0 \times 10^{-5}$ (change in weight for second derivative approximation)
  - $\lambda = 5.0 \times 10^{-7}$ (parameter for regulating the indefiniteness of the Hessian)

3.1. Estimation of the hidden layer neurons

As already stated in Section 2.1 the dataset X used for the experiments is composed of 1164 samples of the EE class, 1160 samples of the SP class and 241 sample of the TT class. The total number of extracted features is $m = 40$. Thus, each element x in the dataset is a row vector of size m. Notice that the number of samples in the TT class is less than the amount of sample in other classes, which means that the X dataset is an *unbalanced dataset*. In this case, it is necessary to process the dataset to obtain a balanced training set for the neural networks.

3.1.1. Estimation for the MCN classifier

The input dataset X was subsampled by using 10 different extraction X_i^0, $i = 1, \ldots, 10$, each of them of size 720, obtaining 10 balanced datasets of 240 elements for each of the classes. For each extracted dataset X_i^0, different versions of the MCN classifier have been considered, each using a different number of neurons K in the hidden layer, in the integer interval $K = [3, 60]$ with steps of 1 neuron. For every value of K, a 10–fold cross validation procedure has been performed. This means that for each value of K, 100 different runs are computed (10 fold on 10 different extracted datasets). The median values of the classifier accuracies have been used to select the number of neurons. In particular, $K = 41$ has been chosen. Fig. 7(a) shows the boxplots of the accuracies for each K, where a red notch represents the median value. It is also possible to observe that increasing the number of neurons does not seem to improve the classification performances. Table 2 shows means and variance of accuracies, mean absolute errors (MAE), mean squared errors (MSE) and Pearson correlation (R) values of the MCN network adopting the selected number of neurons. The sets where the measures have been computed are training, validation and test. The validation set size is 15% of the total training size. The MCN shows an average test accuracy of around 90%.

3.1.2. Estimation for the MBN classifier

To test the efficacy of MBN 30 dataset X_i^h, $i = 1, \ldots, 10$, $h = EE, SP, TT$, were extracted. The reason is always related to the need to avoid an unbalanced training set. Considering that the MBN is the combination of three binary classifiers, each of the single classifier was tested on a group of 10 datasets. In more details, X_i^{EE}, X_i^{SP}, $i = 1, \ldots 10$ are the

datasets used by the binary classifiers B_{EE} and B_{SP} respectively, each composed by 480 elements of positives samples (EE, or SP) and $240 + 240$ negatives samples (SP + TT or EE + TT), obtained by the union of the items belonging to the 2 classes of negative examples. The total number of elements of each dataset X_i^{EE}, X_i^{SP} is 720. The last group of 10 datasets $X_i^{TT} i = 1, \ldots, 10$ are the datasets related to B_{TT}, the classifier for the TT class, that is the class with the lower cardinality (240). Therefore, each of the X_i^{TT} have a size of $|X_i^{TT}| = 480$, where 240 are the positives instances (TT), and $120 + 120$ are the negative instances (from SP + EE classes). Fig. 7 (b,c,d) shows the accuracy of each single classifier B_h, $h = EE, SP, TT$ for each extracted dataset and for each number of neurons K in the hidden layer, again with $K \in [3, 60]$. For each value of K, 100 different runs are computed (10 fold on 10 different extracted datasets). The results indicate a number of neurons for the hidden layer equal to {22,48,21} for the EE, SP, TT classifiers respectively (see Fig. 7(b,c,d)). Also, in this case, the median values of the accuracies have been used. The values of K are set in each B_h, $h = EE, SP, TT$, which are subsequently combined to build the MBN classifier (see Section 2.4 for details about the combination paradigm).

Table 2 shows the means and variance of accuracies, mean absolute errors, mean squared errors and peasron correlation values of the MBN that uses the selected number of hidden units for every single binary classifier. The sets where the measures have been computed are training, validation and test. The result of the test average accuracy is around 88%. The training algorithms of each MBN network are the same as the MCN.

3.1.3. Analysis of the results

A comparison of the results, as reported in Table 2 show that the MCN multiclass has slightly better performances than the MBN network. The final number of hidden units for the two networks are summarized in Table 3. Although the values seem to have an oscillating trend, the lower number of hidden units was selected to obtain the simpler network (a lesser number of hidden units means a lesser number of weights), assuming the same accuracy level.

3.2. Feature selection experiments

The following sections report the results of the feature selection strategies FS and WS for the two classifier architectures. The goal of the experiments is to study the suitable feature selection method. The neural networks have the number of hidden units reported i Table 3.

3.2.1. Using the "filter select" (FS) approach

The FS method has been used setting the value α to 0.8. As already specified, the FS approach works for the case of binary class label assignment and does not make any use of a classifier to rank the features. To apply the FS approach to the MBN classifier three different binary labellings L_h on the input dataset X^h have been considered, so that the label 1 in L_h was related to the items belonging to class h. The application of FS to the dataset X^h produces a ranked list of features I_h. The FS method has been computed on 100 balanced datasets extracted from the input, resulting in a list of 100 ranked features, for each h, stored in

Table 2
The performance obtained by the classifiers with the selected number of hidden units units.

		Accuracy		MAE		MSE		R	
		mean	var	mean	var	mean	var	mean	var
MBN	Training	92,75%	0,08%	0,1269	0,0019	0,0543	0,0005	0,8790	0,0031
	Validation	91,04%	0,13%	0,1440	0,0018	0,0685	0,0005	0,8436	0,0040
	Test	88,20%	0,22%	0,1575	0,0014	0,0799	0,0004	0,8169	0,0028
MCN	Training	93,30%	0,29%	0,0718	0,0032	0,0278	0,0007	0,9344	0,0043
	Validation	91,73%	0,36%	0,0889	0,0031	0,0415	0,0008	0,8996	0,0052
	Test	90,56%	0,29%	0,0939	0,0029	0,0453	0,0007	0,8905	0,0045

S. Aronica et al.

Table 3
The number of hidden units K for each neural network.

		K
MBN	EE	22
	SP	48
	TT	21
MCN		41

a matrix M_h of 100×40 integers in the range $\{1, 40\}$. The resulting selected features S_h have been the ones that appeared at least 55 times in the rankings of the top 55% features. This threshold has been chosen as a reasonable value above the 50%. Table 8 shows in the first columns and first three rows the number of features selected by the FS, for each of the binary classifiers B_h. For the case of *MCN*, a specific strategy for the use FS on a 3 class labelled dataset has been used. This is mandatory taking into account that the FS works only for the case of two label assignment. Let us consider the three different labeling L_h related to the datasets X^h, $h = EE, \ TT, \ SP$. The application of FS to each one of the dataset will create three rankings, I_h, $h = EE, \ TT, \ SP$. The ranking vector J related to the three classes dataset is build iteratively in the following way:

$J = 0/$;

for all$i = 1, \ldots, 40$ **do**

$T = \cap_h [I_h(1),.., I_h(i)] - J$;

$J = [J(1), J(2),..J(i-1), T(1),.., T(N)]$

end for.

where $[I_h(1), I_h(2),.., I_h(i)]$ are the three ranked lists of rank at most i related to every single labelling, N is the cardinality of the set T. The definition of the combination strategy is such that the ranking J is constructed by appending to J, at each iteration i, the new common elements among the three ranked lists with maximum rank i. In this case, the resulting selected features S have been the ones that appeared at least 55 times in the rankings of the top 55% features.

Table 4 lists the features selected by FS. In this table, there is a check (a character" x") if the feature is considered for the corresponding classifier.

Table 5 shows the performance of the *MCN* and *MBN* when using the features selected by FS. The results show an improvement of test

accuracy for *MBN* ($\sim 89\%$ vs 88%) and a decrease of improvements for *MCN* (87% vs 90%) with respect to the simple case of no feature selection in Table 2. Note that the number of features selected by FS is significantly reduced (see Table 8).

3.2.2. Using the "wrapper select" (WS) approach

The WS uses a GA (see before, Section 2.3.2) to search for the best subset of features. The procedure can be applied for the case of *MCN* or *MBN*.

The used GA algorithm adopts the single point crossover as crossover operator and uniform mutation as mutation operator. The selection operator was set to binary tournament. Details about these operators can be found in the book by Michalewicz (Michalewicz, 1996).

The max number of generations of the GA has been set to 30, and the probabilities for crossover (pc) and mutation (pm) have been set to $pc = 0.7$, $pm = 0.05$ respectively.

The fitness function of the *GA* is the accuracy of the relative classifier (*MCN* or the three B_h) computed on a test set.

The GA algorithm was executed 100 times, where a training-test split is produced in each run. In compliance with the previous experimental settings, 10 balanced datasets are extracted, and in each one, a 10 fold cross validation procedure is executed. The classifier that we used is trained on the training set, and the fitness is computed on the test set.

The GA will finally select a list of best chromosomes s^k where each bit s_j^k $j = 1, 2, \ldots 40$ indicates if the corresponding feature j should be considered as input for the MCN classifier ($s_j^k = 1$) or not ($s_j^k = 0$).

3.3. Setting

$$\Gamma(j) = \sum_{k=1}^{100} s_j^k \quad j = 1, \ldots 40 \tag{7}$$

the feature j is selected if $\Gamma(j) > 55$.

For the case of *MBN*, the GA procedure is applied for each of the three classifiers B_h $h = EE, \ SP, \ TT$.

The features selected by *WS* for the three classifiers are reported in Table 6, the symbols in the table have the same meaning of the ones in Table 4.

Table 7 show the performance of the *MCN* and *MBN* when using the features selected by WS. The results show a significant improvement of

Table 4
The list of features selected by FS; the"x" symbol indicates that the corresponding feature was selected as input for the binary classifier of the class EE, SP or TT.

No.	Descriptor	MBN			MCN	2No.	Descriptor	MBN			MCN
		EE	SP	TT				EE	SP	TT	
1	Kurtosis	×	×		×	21	Height_mean				
2	Attack_angle				×	22	Standard_deviation				
3	Corrected_lenght	×			×	23	Skewness				
4	Corrected_thickness					24	Sv_mean				
5	Corrected_perimeter		×	×	×	25	Sv_max				
6	Corrected_area					26	Sv_min				
7	Image_compactness	×	×	×	×	27	Sv_noise				
8	Corrected_mean_amplitude	×	×		×	28	Nasc				
9	Corrected_MVBS					29	ABC	×	×	×	×
10	Coefficient_of_variation					30	Mean_school_depth	×	×	×	×
11	Horizontal_roughness_coefficient		×			31	Bottom_depth	×		×	×
12	Vertical_roughness_coefficient					32	Distance_from_coast			×	
13	3D_school_area					33	Water temperature to 5 m	×		×	×
14	3D_school_volume					34	Water Temperature at bottom			×	
15	Area_Backscatter_Strenght					35	Salinity to 5 m	×	×	×	×
16	Density_number					36	Salinity at bottom	×	×	×	×
17	Density_weight	×		×	×	37	Florescence to 5 m		×	×	
18	Thickness_mean	×				38	Fluorescence at the bottom				
19	Range_mean					39	Oxygen to 5 m	×	×	×	×
20	Beam_volume_sum	×	×		×	40	Oxygen at the bottom		×	×	

Table 5
The performance of the classifiers obtained by using the rank-feature selection (filter approach) method.

		Accuracy		MAE		MSE		R	
		mean	var	mean	var	mean	var	mean	var
MBN	Training	93,17%	0,08%	0,1177	0,0018	0,0509	0,0005	0,8862	0,0032
	Validation	92,15%	0,11%	0,1275	0,0018	0,0593	0,0005	0,8658	0,0034
	Test	89,41%	0,17%	0,1396	0,0016	0,0705	0,0005	0,8392	0,0035
MCN	Training	90,09%	0,46%	0,0923	0,0033	0,0384	0,0008	0,9076	0,0055
	Validation	89,41%	0,49%	0,1095	0,0035	0,0532	0,0010	0,8682	0,0077
	Test	87,32%	0,50%	0,1114	0,0032	0,0548	0,0009	0,8652	0,0067

test accuracies for both *MBN* and *MCN* (~95%) with respect to the previous results in Table 5.

3.3.1. Analysis of the results

The goal of this section is to select the suitable set of features for the two classifiers structure, with the previously elected number of hidden units. ¡by comparing the data in Table 5 and Table 7 it is clear that the best results regarding accuracy are obtained by using the WS approach both on MBN and MCN classifiers. In particular, the accuracy of the two classifiers is almost equal. The total number of features selected is reported in Table 8.

Fig. 8 shows the mean accuracy of the test phase for the two networks MCN and MBN, and the three input features sets: all the features without any selection, features selected by using the FS (filter select) method, and features selected using the WS (wrapper select) method.

3.3.2. Experiments with the OPS class

This set of experiments was carried out to evaluate the proposed model in the case of the presence of the OPS class. Unfortunately, a dataset of the used feature measurements for species different from EE, SP, TT was not available. This limitation is overcomed generating a synthetic species OPS in the following way. Given our dataset X, a matrix Q of size 10×40 random values are extracted from the data matrix which stores X. The values in Q represent the seeds for the generation of synthetic data. The final set of 100 OPS elements are generated such that each feature value $y_i(j)$ is a uniform random value in the interval $[m_j + \sigma_j, U_j] \cup [L_j, m_j - \sigma_j]$ where m_j is the median of the column j in Q, σ_j is its standard deviation and L_j, U_j are minimum and maximum values in column j. This process of random data generation allows us to generate OPS feature samples far enough from the median

value of each feature in j in Q. Finally, the dataset Y is built adding the elements $y_1, \ldots, y_{100}$ to X. Table 9 reports in columns the classifier output and in rows the actual class of the data. This kind of table is often referred to as *confusion matrix* and it is useful to highlights the correctly and misclassified data. In particular, it shows the classification rates of each class for the test set data, averaged on 10 fold, using a 10 fold cross validation procedure. The total accuracy, computed as the sum of the value in the matrix diagonal, is around 96%.

4. Discussion

The used classifiers perform quite equally using the *WS* approach. In the end, due to the unique property of the MBN to recognize an unknown class, makes it preferable to MCN. Its performances are improved with respect to the 88% of accuracy reached by the networks with no feature selection, and also concerning the accuracy using the FS approach as feature selection. Fig. 9 shows the final MBN classifier. It is possible to observe that each binary classifier used for the combination adopts a different set of features. Each set is the result of the *wrapper–select* algorithm applied to the related binary classifier. The results in Table 3.3 indicate that the MBN classifier can accurately identify EE schools in 95% of cases using only 12 of the available features, the SP in 94% of cases using 18 features while TT in ~97% of cases using only other 11 features. Moreover, MBN was also able to recognize 97% of OPS cases, which is specified in the paragraph 3.3 and is relative to data generated synthetically.

In Table 3 the features indicated by numbers from 33 to 40 are related to water conditions (temperature, salinity and so on), and most of these features are selected by the WS procedure as input for the binary classifiers. It also seems that the variables related to

Table 6
The list of features selected by WS; the "x" symbol indicates that the corresponding feature was selected as input for the binary classifier of the class EE, SP or TT.

No.	Descriptor	MBN			MCN	No.	Descriptor	MBN			MCN
		EE	SP	TT				EE	SP	TT	
1	Kurtosis					21	Height_mean				×
2	Attack_angle				×	22	Standard_deviation		×		×
3	Corrected_lenght			×		23	Skewness				
4	Corrected_thickness					24	Sv_mean				×
5	Corrected_perimeter			×	×	25	Sv_max				×
6	Corrected_area		×			26	Sv_min		×		
7	Image_compactness					27	Sv_noise				×
8	Corrected_mean_amplitude					28	Nasc				×
9	Corrected_MVBS	×			×	29	ABC				
10	Coefficient_of_variation					30	Mean_school_depth		×		×
11	Horizontal_roughness_coefficient	×				31	Bottom_depth	×	×	×	×
12	Vertical_roughness_coefficient		×		×	32	Distance_from_coast	×	×	×	×
13	3D_school_area				×	33	Water temperature to 5 m	×	×	×	×
14	3D_school_volume		×			34	Water Temperature at bottom	×	×	×	×
15	Area_Backscatter_Strenght					35	Salinity to 5 m	×	×		×
16	Density_number		×			36	Salinity at bottom	×		×	×
17	Density_weight		×			37	Florescence to 5 m	×	×	×	×
18	Thickness_mean			×		38	Fluorescence at the bottom	×	×	×	×
19	Range_mean		×	×		39	Oxygen to 5 m	×	×	×	×
20	Beam_volume_sum					40	Oxygen at the bottom	×	×	×	×

Table 7
The performance obtained with the features selected by using the wrapper method (using a GA).

		Accuracy		MAE		MSE		R	
		mean	var	mean	var	mean	var	mean	var
MBN	Training	96,99%	0,06%	0,0457	0,0013	0,0176	0,0003	0.9619	0.0017
	Validation	96,80%	0,06%	0,0566	0,0012	0,0254	0,0003	0,9456	0,0016
	Test	94,90%	0,15%	0,0636	0,0013	0,0323	0,0003	0.9298	0.0021
MCN	Training	96,26%	0,18%	0,0408	0,0016	0,0136	0,0003	0,9687	0,0018
	Validation	95,32%	0,18%	0,0545	0,0016	0,0239	0,0004	0,9437	0,0026
	Test	93,99%	0,23%	0,0555	0,0014	0,0251	0,0003	0,9414	0,0018

Table 8
The number of features selected by the two methods.

		No. Features	
		FS	WS
MBN	EE	15	12
	SP	13	18
	TT	14	11
MCN		15	24

Table 9
The rate confusion matrix of the classifier.

	OPS	EE	SP	TT
OPS	97,09%	2,91%	0	0
EE	2,33%	95,35%	2,33%	0
SP	0.38%	5,13%	94,49%	0
TT	0.44%	2,72%	0	96,84%

temperature, fluorescence and oxygen to 5 m are useful for every single binary classifier.

There are several studies that in different ways (MLP, SVM, PNN, Classification Tree, etc.) and for different species (anchovy, sardines, horse mackerel, capelin, polar cod, herring, Norway pout and more) have dealt with the pelagic species identification problem by taking both the species ecology and behavior into account (Fernandes, 2009; McClatchie et al., 2000; Fernandes et al., 2006; Fässler et al., 2007). However, they do not seem as effective as the one that we propose here. Our belief is that the difference is due to the adoption of additional ecological features, and to the adopted feature selection process. This procedure has lowered the number of input variables for the neural network, from the initial 40 to just over a third of them.

Of course, it would be very interesting to extend this work even in environments where there are multispecies fish schools in which the variability of the composition of the same does not constitute a limitation.

5. Conclusions

A reliable evaluation of marine fish resources is very important for planning fisheries management actions, which may support the sustainable exploitation of such resources, and for ensuring not only the

conservation of biodiversity but also the protection of fish resources. However, this assessment for small pelagic fishes is not a simple task and can be obtained through both the monitoring of fishery landings (fishery dependent data) and the acoustic evaluation through scientific surveys at sea (fishery independent sources). While monitoring landings can give an estimation of fish biomass taken from the sea, acoustic surveys can give an idea of the total biomass present in the surveyed area.

Consequently, an accurate estimation of abundance and distribution of small pelagics in a given sea area can permit more accurate management plans. In this context, the present study aimed to improve the procedures of species identification of the insonified pelagic fish schools. The results of our experiments have suggested a classification scheme that uses a combination of binary classifiers, each one adopting a specific subset of features indicated by the wrapper approach. The performance of the classifier suggests that it is capable of taking advantage of the acoustic and environmental features. One of the advantages of the classifier is that it can also determine if a fish school does not belong to one of the three considered species. This special behaviour could be useful when future devices will be designed to help fishermen to improve the selectivity of their fishery activity, thus reducing by-catches. The methodology adopted for the classification of small pelagic schools shows that environmental features are of some importance. This result is corroborated by the results obtained by
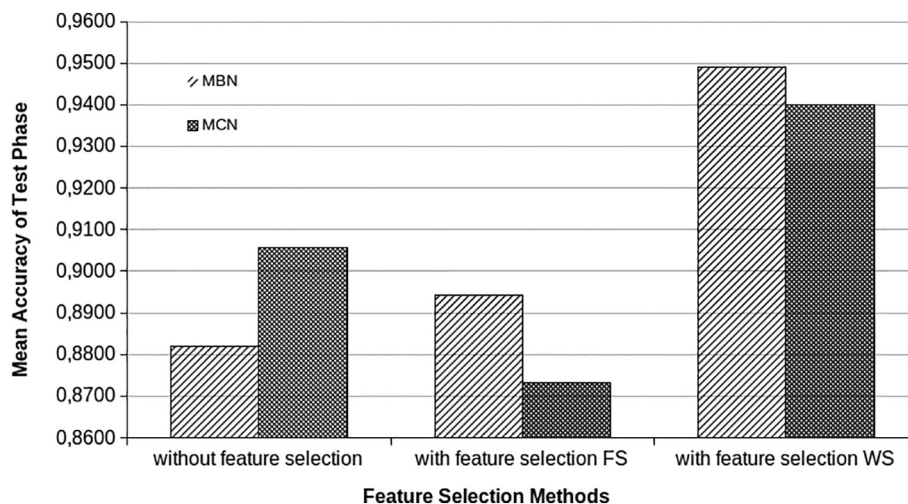
Fig. 8. The mean accuracy obtained for the three configuration of input features.

Table 10
Description of the parameters.

Parameter	Description
Kurtosis	Kurtosis (dB re $1 \, \text{m}^{-1}$) is a statistic that is used to measure the" flatness" or" peakedness" of a set of data.
Attack_angle	Diner in (Diner, 2001) defines the attack angle as "the angle between a vertical line, from the transducer, and another line, towards the school edge, measured at the moment when the school detection is just beginning".
Corrected length	Corrected length (m) reports the Uncorrected length corrected for known beam geometry, according to (Diner, 2014).
Corrected_thickness	Corrected thickness (m) reports the Uncorrected thickness corrected for known beam geometry, according to (Diner, 2014).
Corrected_perimeter	Corrected perimeter (m) reports the Uncorrected perimeter corrected for known beam geometry according to the system of Diner (Diner, 2014).
Corrected_area	Corrected area (m^2) reports the Uncorrected area corrected for known beam geometry according to the system of (Diner, 2014).
Image_compactness	Image compactness is a statistics, which measures the ratio between the squared perimeter and the area of the observed school. A circle has an image compactness of 1.
Corrected_mean amplitude	Corrected mean amplitude (m^2/m^3) reports the linear mean Sv of a school represented by a region on an echogram corrected for known beam geometry according to (Diner, 2014).
Corrected_MVBS	Corrected MVBS (dB re $1 \, \text{m}^2/\text{m}^3$) reports the value of Corrected mean amplitude in the dB domain. This is a representation of the mean Sv of a school represented by a region on an echogram corrected for known beam geometry according to (Diner, 2014).
Coefficient_of variation	Coefficient of variation (%) reports the coefficient of variation of the Sv values in a school represented by a region on an echogram.
Horizontal_roughness coefficient	The horizontal roughness coefficient (dB re $1 \, \text{m}^2/\text{m}^3$) is a statistics used to measure the dispersion of acoustic energy within the school in the horizontal direction. This provides an index of the distribution of more and less dense patches within the school and/or of larger and smaller individuals (fish) within the school.
Vertical_roughness coefficient	The vertical roughness coefficient (dB re $1 \, \text{m}^2/\text{m}^3$) is a statistics used to measure the dispersion of acoustic energy within the school in the vertical direction. This provides an index of the distribution of more and less dense patches within the school and/or of larger and smaller individuals (fish) within the school.
3D_school_area	3D school area (m^2) reports the estimated surface area of a school represented by a region on an echogram, assuming that it is cylindrical.
3D_school_volume	3D school volume (m^3) reports the estimated volume of a school represented by a region on an echogram, assuming it is cylindrical.
Area_backscatter strength	Area backscatter strength (m^2/nmi^2) reports the Area Backscatter Strength for the domain that was analyzed. This is a logarithmic representation of the ABC value.
Density_number	Density number (fish/nmi^2 or fish/ha) reports the number of fish per unit area for the domain that was analyzed.
Density_weight	Density weight (kg/nmi^2 or kg/ha) reports the weight of fish per unit area for the domain that was analyzed.
Thickness_mean	Thickness mean (m) reports the mean thickness of the domain that was analyzed. A measure of the extent of an object (specifically a region, cell, region-cell intersection or selection), along the beam axis.
Range_mean	Range mean (m) is an analysis variable representing the mean range of an object from the transducer face.
Beam_volume_sum	Beam volume sum (m^3) reports the sum of the beam volumes of all pings in the domain that was analyzed.
Height_mean	Height mean (m) reports the mean height of the domain that was analyzed.
Standard_deviation	Standard deviation reports the standard deviation of all sample values in the domain that was analyzed.
Skewness	Skewness is a statistics that is used to measure the symmetry of the distribution for a set of data. A distribution that is skewed tails off to the left or to the right (dB re $1 \, \text{m}^{-1}$).
Sv_mean	Sv mean (dB re $1 \, \text{m}^{-1}$) reports the mean Sv in the domain that was analyzed.
Sv_max	Sv max (dB re $1 \, \text{m}^{-1}$) reports the maximum Sv in the domain that was analyzed.
Sv_min	Sv min (dB re $1 \, \text{m}^{-1}$) reports the maximum Sv in the domain that was analyzed.
Sv_noise	Sv noise (dB re $1 \, \text{m}^{-1}$) reports the mean noise Sv in the domain that was analyzed.
Nasc	The Nautical Area Scattering Coefficient (m^2/nmi^2) for the domain that was analyzed (MacLennan et al., 2002).
ABC	ABC (m^2/nmi^2) reports the Area backscattering coefficient for the domain that was analyzed (MacLennan et al., 2002).
Mean school depth	The mean depth (m) of the school in the water column.
Maximum vertical linking distance	This is the maximum vertical distance allowed between two school candidates being linked to form a school.
Maximum horizontal linking distance	This is the maximum horizontal distance allowed between two school candidates being linked to form a school.
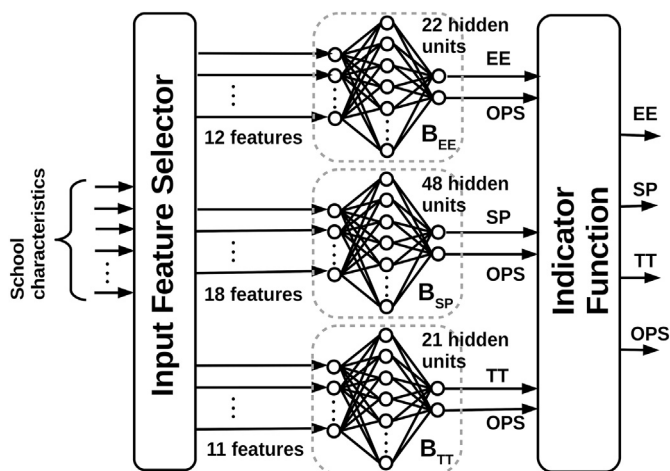
Fig. 9. The scheme of the model adopted to automatically classify the three species. The input feature selector is the set of wiring that takes the suitable set of features to each classifier of the structure. The Indicator Function is the *argmax* function described in Section 2.4.

Bonanno et al. (Bonanno et al., 2014) in the Strait of Sicily and in the Aegean Sea. The authors studying the habitat suitability of anchovies and sardines have highlighted environmental ranges favorable to the two species. The results of this work, which also take into consideration a third species (*Trachurus trachurus*), seem to be promising and applicable also in other areas of the Mediterranean Sea.

Acknowledgements

References

Barange, M., 1994. Acoustic identification, classification and structure of biological patchiness on the edge of the agulhas bank and its relation to frontal features. S. Afr. J. Mar. Sci. 14, 333–347.

Barra, M., Petitgas, P., Bonanno, A., Somarakis, S., Woillez, M., Machias, A., Mazzola, S., Basilone, G., Giannoulaki, M., 2015. Interannual changes in biomass affect the spatial aggregations of anchovy and sardine as evidenced by geostatistical and spatial indicators. PLoS One 10, e0135808.

Basilone, G., Mangano, S., Pulizzi, M., Fontana, I., Giacalone, G., Ferreri, R., Gargano, A., Aronica, S., Barra, M., Genovese, S., et al., 2017. European anchovy (*Engraulis encrasicolus*) age structure and growth rate in two contrasted areas of the mediterranean sea: the paradox of faster growth in oligotrophic seas. Mediterr. Mar. Sci. 504–516.

Basilone, G., Ferreri, R., Mangano, S., Pulizzi, M., Gargano, A., Barra, M., Mazzola, S., Fontana, I., Giacalone, G., Genovese, S., Aronica, S., Bonanno, A., 2018. Effects of habitat conditions at hatching time on growth history of offspring european anchovy, *Engraulis encrasicolus*, in the central mediterranean sea. Hydrobiologia 821, 99–111.

Bonanno, A., Giannoulaki, M., Barra, M., Basilone, G., Machias, A., Genovese, S., Goncharov, S., Popov, S., Rumolo, P., Di Bitetto, M., Aronica, S., Patti, B., Fontana, I., Giacalone, G., Ferreri, R., Buscaino, G., Somarakis, S., Pyrounaki, M.M., Tsoukali, S., Mazzola, S., 2014. Habitat selection response of small pelagic fish in different environments. Two examples from the oligotrophic Mediterranean Sea. PLoS One 9 (7), e101498.

Bonanno, A., Zgozi, S., Basilone, G., Hamza, M., Barra, M., Genovese, S., Rumolo, P., Nfate, A., Elsger, M., Goncharov, S., et al., 2015. Acoustically detected pelagic fish community in relation to environmental conditions observed in the central mediterranean sea: a comparison of libyan and Sicilian–maltese coastal areas. Hydrobiologia 755, 209–224.

Bonanno, A., Barra, M., Basilone, G., Genovese, S., Rumolo, P., Goncharov, S., Popov, S., Buongiorno Nardelli, B., Iudicone, D., Procaccini, G., et al., 2016. Environmental processes driving anchovy and sardine distribution in a highly variable environment: the role of the coastal structure and riverine input. Fish. Oceanogr. 25, 471–490.

Bonanno, A., Barra, M., Mifsud, R., Basilone, G., Genovese, S., Di Bitetto, M., Aronica, S., Giacalone, G., Fontana, I., Mangano, S., Ferreri, R., Pulizzi, M., Rumolo, P., Gargano, A., Buscaino, G., Calandrino, P., Di Maria, A., Mazzola, S., 2018. Space utilization by key species of the pelagic fish community in an upwelling ecosystem of the mediterranean sea. Hydrobiologia 821, 173–190.

Brankart, J., 1994. The Modb Local Quality Control, Technical Report. University of Liège, pp. 5.

Cabreira, G., Arial, M., Tripode, Madirolas, 2009. Artificial neural networks for fish-species identification. ICES J. Mar. Sci. 66, 1119–1129.

Campanella, F., Taylor, J.C., 2016. Investigating acoustic diversity of fish aggregations in coral reef ecosystems from multifrequency fishery sonar surveys. Fish. Res. 181, 63–76.

Charef, A., Ohshimo, S., Aoki, I., Al Absi, N., 2010. Classification of fish schools based on evaluation of acoustic descriptor characteristics. Fish. Sci. 76, 1–11.

Cooke, J., 1984. Glossary of technical terms. In: Exploitation of Marine Communities, (rm may, Ed.).

Crawford, R., 1987. Food and population variability in five regions supporting large stocks of anchovy, sardine and horse mackerel. S. Afr. J. Mar. Sci. 5, 735–757.

Cury, P., Bakun, A., Crawford, R.J., Jarre, A., Quinones, R.A., Shannon, L.J., Verheye, H.M., 2000. Small pelagics in upwelling systems: patterns of interaction and structural changes in "wasp-waist" ecosystems. ICES J. Mar. Sci. 57, 603–618.

Cury, P., Shannon, L., Shin, Y.-J., 2003. The Functioning of Marine Ecosystems: A Fisheries Perspective, Responsible Fisheries in the Marine Ecosystem. pp. 103–123.

De Robertis, A., Higginbottom, I., 2007. A post-processing technique to estimate the signal-to-noise ratio and remove echosounder background noise. ICES J. Mar. Sci. 64, 1282–1291.

D'Elia, M., Patti, B., Bonanno, A., Fontana, I., Giacalone, G., Basilone, G., Fernandes, P., 2014. Analysis of backscatter properties and application of classification procedures for the identification of small pelagic fish species in the central mediterranean. Fish. Res. 149, 33–42.

Demer, D.A., Cutter, G.R., Renfree, J.S., Butler, J.L., 2009. A statistical- spectral method for echo classification. ICES J. Mar. Sci. 66, 1081–1090.

Diner, N., 2001. Correction on school geometry and density: approach based on acoustic image simulation. Aquat. Living Resour. 14, 211–222.

Diner, N., 2014. Correction on School Geometry and Density. ICES C.M. /B:1).

FAO, GFCM, 2016. The State of Mediterranean and Black Sea Fisheries. FAO, Rome.

Fässler, S.M., Santos, R., García-Núñez, N., Fernandes, P.G., 2007. Multifrequency backscattering properties of Atlantic herring (*Clupea harengus*) and Norway pout (*Trisopterus esmarkii*). Can. J. Fish. Aquat. Sci. 64, 362–374.

Fernandes, P.G., 2009. Classification trees for species identification of fish- school echotraces. ICES J. Mar. Sci. 66, 1073–1080.

Fernandes, P., Korneliussen, R., Lebourges-Dhaussy, A., Masse, J., Iglesias, M., Diner, N., Ona, E., Knutsen, T., Gajate, J., Ponce, R., 2006. The SIMFAMI Project: Species Identification Methods from Acoustic Multifrequency Information, Final Report to the EC. Q5RS–2001–02054.

Fontana, I., Giacalone, G., Bonanno, A., Mazzola, S., Basilone, G., Genovese, S., Aronica, S., Pissis, S., Iliopoulos, C., Kundu, R., et al., 2017. Pelagic species identification by using a pnn neural network and echo-sounder data. Lect. Notes Comput. Sci 10613, 454–455.

Gascuel, D., 2005. The trophic-level based model: a theoretical approach of fishing effects on marine ecosystems. Ecol. Model. 189, 315–332.

Guyon, I., Elisseeff, A., 2003. An introduction to variable and feature selection. J. Mach. Learn. Res. 3, 1157–1182.

Higginbottom, I., 2000. Virtual echograms for visualisation and postprocessing of multiple-frequency echosounder data. In: Proceedings of the Fifth European Conference on Underwater Acoustics, ECUA. July. Lyon, France.

Horne, J.K., 2000. Acoustic approaches to remote species identification: a review. Fish. Oceanogr. 9, 356–371.

Hornik, K., Stinchcombe, M., White, H., 1989. Multilayer feedforward networks are universal approximators. Neural Netw. 2, 359–366.

Huan, L., Motoda, H., 1998. Feature Selection for Knowledge Discovery and Data Mining. Springer.

Jackson, J.B., Kirby, M.X., Berger, W.H., Bjorndal, K.A., Bots- ford, L.W., Bourque, B.J., Bradbury, R.H., Cooke, R., Erlandson, J., Estes, J.A., et al., 2001. Historical overfishing and the recent collapse of coastal ecosystems. Science 293, 629–637.

Kang, N., 2011. Analysis of the ME70 multibeam echosounder data in echoview - current capability and future directions. J. Mar. Sci. Technol. 19 (3), 312–321.

Kloser, R.J., Ryan, T., Sakov, P., Williams, A., Koslow, J.A., 2002. Species identification in deep water using multiple acoustic frequencies. Can. J. Fish. Aquat. Sci 59 (6), 1065–1077.

Kohavi, R., John, G.H., 1997. Wrappers for feature subset selection. Artif. Intell. 97, 273–324.

Lawson, G.L., Barange, M., Fréon, P., 2001. Species identification of pelagic fish schools on the south african continental shelf using acoustic descriptors and ancillary information. ICES J. Mar. Sci. 58, 275–287.

Lleonart, J., Maynou, F., 2003. Fish Stock Assessments in the Mediterranean: State of the Art.

Martignac, F., Daroux, A., Bagliniere, J.L., Ombredame, D., Guillard, J., 2015. The use of acoustic cameras in shallow waters: new hydroacoustic tools for monitoring migratory fish population. A review of didson technology. Fish Fish. 16 (3), 486–510.

McClatchie, S., Thorne, R.E., Grimes, P., Hanchet, S., 2000. Ground truth and target identification for fisheries acoustics. Fish. Res. 47, 173–191.

MEDIAS-Handbook, 2015. Common Protocol for the Pan-Mediterranean Acoustic Survey (medias), Handbook of Mediterranean Acoustic international Acoustic Surveys. March 2015 Available Online. http://www.medias-project.eu/medias/website/handbooks-menu/handbooks/MEDIAS-Handbook-March-2015.pdf/ pp. 21.

Michalewicz, Z., 1996. Genetic Algorithms + Data Structures = Evolution Programs (3rd Ed.). Springer-Verlag, Berlin, Heidelberg.

Morote, E., Olivar, M.P., Villate, F., Uriarte, I., 2008. Diet of round sardinella, sardinella aurita, larvae in relation to plankton availability in the nw mediterranean. J. Plankton Res. 30, 807–816.

Palomera, I., Olivar, M.P., Salat, J., Sabatés, A., Coll, M., García, A., Morales-Nin, B., 2007. Small pelagic fish in the nw mediterranean sea: an ecological review. Prog. Oceanogr. 74, 377–396.

Pauly, D., Christensen, V., Dalsgaard, J., Froese, R., Torres, F., 1998. Fishing down marine food webs. Science 279, 860–863.

Pauly, D., Christensen, V., Guénette, S., Pitcher, T.J., Sumaila, U.R., Walters, C.J., Watson, R., Zeller, D., 2002. Towards sustainability in world fisheries. Nature 418, 689.

Petitgas, P., Massé, J., Beillois, P., Lebarbier, E., Le Cann, A., 2003. Sampling variance of species identification in fisheries acoustic surveys based on automated procedures associating acoustic images and trawl hauls. ICES J. Mar. Sci. 60, 437–445.

Preciado, I., Velasco, F., Olaso, I., 2008. The role of pelagic fish as forage for the demersal fish community in the southern Bay of Biscay. J. Mar. Syst. 72, 407–417.

Reid, D.G., 1999. Report on echo trace classification. A comprehensive review of the state-of-the-art and directions for future research. ICES Cooperative Research Report 238, 107.

Robotham, H., Bosch, P., Gutiérrez-Estrada, J.C., Castillo, J., Pulido- Calvo, I., 2010. Acoustic identification of small pelagic fish species in Chile using support vector machines and neural networks. Fish. Res. 102, 115–122.

Rumolo, P., Bonanno, A., Barra, M., Fanelli, E., Calabrò, M., Genovese, S., Ferreri, R., Mazzola, S., Basilone, G., 2016. Spatial variations in feeding habits and trophic levels of two small pelagic fish species in the Central Mediterranean Sea. Mar. Environ. Res. 115, 65–77.

Rumolo, P., Basilone, G., Fanelli, E., Barra, M., Calabrò, M., Genovese, S., Gherardi, S., Ferreri, R., Mazzola, S., Bonanno, A., 2017. Linking spatial distribution and feeding behavior of Atlantic horse mackerel (*Trachurus trachurus*) in the Strait of Sicily (Central Mediterranean Sea). J. Sea Res. 1211, 47–58.

Rumolo, P., Fanelli, E., Barra, M., Basilone, G., Genovese, S., Gherardi, S., Ferreri, R., Gargano, A., Mazzola, S., Bonanno, A., 2018. Trophic relationships between anchovy (*Engraulis encrasicolus*) and zooplankton in the Strait of Sicily (Central Mediterranean Sea): a stable isotope approach. Hydrobiologia 821, 41–56.

Scalabrin, C., 1991. Recherche d'une méthodologie pour la classification et l'identification automatiques des détections acoustiques des bancs de poissons. Rapp. IFREMER, DITVNP A 91. Vol. 23.

Scalabrin, C., Massé, J., 1993. Acoustic detection of the spatial and temporal distribution of fish shoals in the Bay of Biscay. Aquat. Living Resour. 6, 269–283.

Schwartzlose, R., Alheit, J., 1999. Worldwide large-scale fluctuations of sardine and anchovy populations. Afr. J. Mar. Sci. 21.

Simmonds, J., MacLennan, D.N., 2008. Fisheries Acoustics: Theory and Practice. John Wiley & Sons.

Theodoridis, S., Koutroumbas, K., 2008. Pattern Recognition, 4th Edition. Academic Press.

Tsagarakis, K., Giannoulaki, M., Pyrounaki, M.M., Machias, A., 2015. Species identification of small pelagic fish schools by means of hydroacoustics in the eastern mediterranean sea. Mediterr. Mar. Sci. 13 (1), 151–161.

Tsai, C.-F., Eberle, W., Chu, C.-Y., 2013. Genetic algorithms in feature and instance selection. Knowl.-Based Syst. 39, 240–247.

Valenti, D., Denaro, G., La Cognata, A., Spagnolo, B., Bonanno, A., Basilone, G., Mazzola, S., Zgozi, S., Aronica, S., 2012. Picophytoplankton dynamics in noisy marine environment. Acta Phys. Pol. B 43 (5), 1227–1240.